JOURNAL

OF THE AMERICAN CHEMICAL SOCIETY



VOLUME 106, NUMBER 10 MAY 16, 1984

# $^1$H NMR Spectral Patterns of Rapidly Flipping Tyrosyl Rings: A Study of Crambin in Organic Solvents

**Juliette T. J. Lecomte and Miguel Llinás***

*Contribution from the Department of Chemistry, Carnegie-Mellon University, Pittsburgh, Pennsylvania 15213.* *Received October 6, 1983*

**Abstract:** Crambin, a hydrophobic protein of 4715 $M_r$, readily dissolves in a variety of organic solvent systems while preserving its globular structure. The two tryosyl residues occurring in crambin have been studied by $^1$H NMR spectroscopy at 300 and 600 MHz as a function of solvent composition and temperature. The NMR spectra are consistent with the crystallographic structure which shows that, while the side chain of Tyr$^{29}$ is exposed, the Tyr$^{44}$ aromatic ring is surrounded by a number of amino acid residues. In particular, it is observed that the Tyr$^{29}$ spectral pattern, which corresponds to an AA'XX' spin system, is typical of an unconstrained phenolic ring, as found for such residues in short, flexible oligopeptides. In contrast, Tyr$^{44}$ exhibits an AA'BB' spectrum which can easily degenerate to a singlet or even present a reversed ortho-meta resonance ordering, depending on the solvent in which the protein is dissolved. Thus, of the two tyrosines, the one that structurally is the least exposed is the most sensitive to solvent perturbations. However, a temperature rise consistently drives the Tyr$^{44}$ aromatic spectrum toward assuming the "random coil" characteristics, whichever the solvent. It is concluded that, as found for other proteins, tyrosyl H2,6 and H3,5 phenolic resonances can be distinguished and identified only from the response of the chemical shifts to external perturbations (temperature, pH, etc.) and not from the spectral pattern under fixed conditions. Lanthanide ions and acid-base titration studies in 3:2 acetone/water show that metal binding and pH can lead the Tyr$^{44}$ spectrum to show characteristics it exhibits in other solvents. These experiments suggest that the electrostatic field arising from the neighbor $\gamma$-carboxyl of Asp$^{43}$ is unlikely to be important in determining the Tyr$^{44}$ spectral pattern. The Tyr$^{44}$ ring has previously been shown by $^1$H-{$^1$H} Overhauser experiments to be in close dipolar contact with the two methyl groups of Ile$^{33}$. Correlations between the Ile$^{33}$ $\delta$-methyl resonance shielding and the Tyr$^{44}$ aromatic chemical shifts indicate that packing of the ring by proximal residues is probably the dominant factor controlling the Tyr$^{44}$ phenol spectral pattern. A thermodynamic analysis of the data in terms of a two-state model leads to qualitative predictions regarding the extent of stabilization afforded by most solvent systems; such relative structural stabilization finds in this view a temperature equivalent given by $T_c$, the compensation temperature. For ethanol/acetic acid solvent mixtures the approach proves to be inadequate, an observation which suggests that the variation of the NMR chemical shift in the temperature range explored does not probe a first-order transition implicit in the two-state analysis. Therefore, it is proposed that the temperature dependencies of protein chemical shifts can result from thermal population of higher vibrational levels that sense anharmonic terms of the normal mode potentials and not necessarily from equilibria between folded and unfolded forms of the protein. It is concluded that NMR spectroscopy can monitor the structural dynamics that characterizes the predenaturation temperature range and the internal motions that contribute to the native protein heat capacity.

## Introduction

A most studied section of protein $^1$H NMR spectra is the low-field region, ranging between ~6 and ~10 ppm, that contains histidyl and aromatic side-chain resonances. After removing the amide NH resonances by hydrogen exchange against solvent deuterium, the $\delta \gtrsim 6$ ppm region defines a spectroscopic area which is well separated from the crowded aliphatic region and thence is amenable to selective manipulations of the spin systems by means of double-resonance NOE[1] or spin-decoupling experiments, chemical modification, pH titration, temperature variation, etc. However, except for the acid–base response of titratable side chains, little is known regarding interpretation of aromatic spectral patterns, which often exhibit well-dispersed resonances rich in dynamic information. In order to gain structural insights from the resonance frequencies, compounds are needed that contain aromatic residues in topologically well-defined environments so that any correspondence between chemical shift patterns and molecular conformation can be more clearly discerned.

Crambin is a 4715-dalton, water-insoluble protein of 46 amino acid residues in a chain constrained by three disulfide bridges.[2,3] As isolated, the protein is heterogeneous, with substitutions at sites 22 and 25.[3,4] Its crystallographic structure has been solved by

(1) Abbreviations used: NOE, nuclear Overhauser effect; pH*, glass electrode pH reading uncorrected for solvent or isotope effects; ppm, parts per million; $Me_4Si$, tetramethylsilane; DOAc, [$^2H_4$]acetic acid; EtOD, [$^2H_4$]-ethanol; DMF, [$^2H_7$]dimethylformamide; TFE, [$^2H_3$]trifluoroethanol; acetone, [$^2H_6$]acetone; $D_2O$, $^2H_2O$.

(2) Van Etten, C.H.; Nielsen, H. C.; Peters, J. E. *Phytochemistry* **1965**, *4*, 467–473.

(3) Teeter, M. M.; Mazer, J. A.; L'Italien, J. J. *Biochemistry* **1981**, *20*, 5437–5443.

(4) Hendrickson, W. A.; Teeter, M. M. *Nature (London)* **1981**, *290*, 107–113.

0002-7863/84/1506-2741$01.50/0 

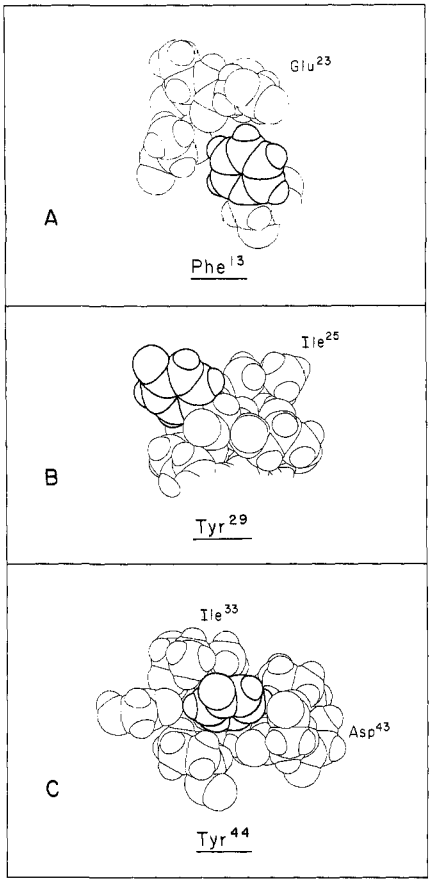


**Figure 1.** Aromatic residues of crambin:[4] the environments of $Phe^{13}$ (A), $Tyr^{29}$ (B), and $Tyr^{44}$ (C). Relevant residues discussed in the text are labeled.

direct methods to 1.5-Å resolution[4] and is presently under refinement by the original authors. Because of its hydrophobilicity, organic solvent systems of different properties were explored in order to solubilize the protein for high-resolution NMR studies.[5-7] In the course of such investigations, we observed that the $Tyr^{44}$ aromatic spectrum, averaged to an AA'BB' pattern characteristic of a freely flipping ring, shows a strong solvent dependence while the two doublets corresponding to $Tyr^{29}$ signals, typical of a "random coil" or structurally unconstrained side chain, exhibit negligible response to solvent changes. The crystallographic structure[4] shows $Tyr^{29}$ to be exposed (Figure 1B), its side chain extending out of a regular $\alpha$-helix that goes from residue 23 to 31. In contrast, $Tyr^{44}$ is more protected, sandwiched between $Asp^{43}$ and $Ile^{33}$ (Figure 1C). Thus, it is surprising that while the $Tyr^{29}$ signals show little solvent-induced shifts, $Tyr^{44}$, sterically more shielded, appears to be so sensitive to the media.

Because in many of the media initially tested crambin exhibited limited solubility and often resulted in broad-line spectra[5] reflecting aggregation of the protein, some of these solvents (e.g., trifluoroethanol, acetone/water mixtures, etc.) have been reexamined as we have more recently found that at concentrations ~1 mM crambin often yields satisfactorily narrow NMR resonances. In this paper, we address ourselves to the problem of tyrosyl ring $^1H$ NMR spectral patterns using crambin as a model system on which both temperature and solvent composition can be widely varied. The changes in the $Tyr^{44}$ spectrum are discussed and compared with the effects on the $Ile^{33}$ $CH_3^{\delta}$ resonance in order to ascertain possible interactions between these two proximal groups.

A second problem of interest is the thermostability of native crambin in the different media. The Gibbs free energy of denaturation at 298 K, also called "macro-stability"[8] of the protein, characterizes a transition involving the macromolecule as a single entity. However, proteins may also be viewed as a collection of somewhat independent units, able to unfold transiently; in order to account for the motions which cause native proteins to expose their different consituents and undergo distinct reactions with the medium,[9,10] dynamic modelling is required.[11] Privalov[8] has calculated "micro-stabilities" that characterize such processes for several proteins. Similarly, the denatured form of the protein cannot be assumed to be static, and it follows that both random and native polypeptides show a temperature dependence. Therefore, events occurring outside the denaturation transition range are linked to the heat capacity of the macromolecule and cannot be associated with a cooperative process. Since crambin exhibits a pronounced thermal stability in various solvents, it provides an ideal system to study predenaturational changes occurring in the NMR spectrum as the solution is heated. In particular, $Tyr^{44}$ and $Ile^{33}$ afford good NMR reporter groups owing to their marked sensitivity to the medium. An attempt is presented here to analyze the chemical shift patterns of these two probes in terms of thermal equilibrium between two states.

## Experimental Section

Crambin was extracted from dehulled seeds of *Crambe abyssinica* and purified and crystallized essentially following the procedure of Van Etten et al.[2] The seeds were provided by Dr. H. L. Tookey (Northen Regional Research Center, U.S. Department of Agriculture, Peoria, IL). Lanthanide salts were purchased from ICN Pharmaceuticals, Inc. Deuterated solvents for the NMR experiments originated from Merck Sharp & Dohme, Canada, and were used without further purification, except for $d_6$-acetic acid which was distilled.

Fourier proton NMR spectra were recorded at 300 MHz using a Bruker WM-300 spectrometer, and at 600 MHz using the National Institutes of Health NMR Facility for Biomedical Research at Carnegie-Mellon University. Spectra were resolution enhanced with Gaussian multiplication.[12,13] Temperature was monitored by recording ethylene glycol[14] and methanol[15] spectra. Chemical shifts are given in ppm and are referred to internal $Me_4Si$. Amide and other labile protons were exchanged against solvent deuterons before recording the spectra. Sample concentrations were typically ~1.3 mM.

The molecular model representations in Figure 1 were generated from the crystallographic coordinates of crambin[4] (Brookhaven Protein Data Bank) using PROPHET graphics (Bolt, Beranek & Newman, Inc., Cambridge, MA).

## Results

The four carbon-bound aromic hydrogens of a freely flipping, structurally unconstrained, tyrosyl ring yield, at pH <9, a $^1H$ NMR spectrum consisting of two doublets at ~7.25 and ~6.75 ppm that correspond to pairs of ortho (H2 and H6) and meta (H3 and H5) protons, respectively.[16,17] That two, rather than four, resonances are observed is due to fast averaging on the NMR time scale of the individual proton chemical shifts within each of the H2.6 and H3.5 pairs to yield a characteristic AA'XX' spectral pattern. However, even if there is rapid thermal ring flipping, in the case of globular proteins of compact structure the pattern can noticeably deviate from the "random coil" AA'XX' case described above. This is so simply because the chemical shifts

(5) Llinás, M.; De Marco, A.; Lecomte, J. T. J. *Biochemistry* **1980**, *19*, 1140–1145.
(6) De Marco, A.; Lecomte, J. T. J. Llinás, M. *Eur. J. Biochem.* **1981**, *119*, 483–490.
(7) Lecomte, J. T. J.; Llinás, M. *Biochemistry*, in press.
(8) Privalov, P. L.; Tsalkova, T. N. *Nature (London)* **1979**, *280*, 693–696.
(9) Linderstrøm-Lang, K. U. In "Proceedings of the Symposium on Protein Structure"; Neuberger, A., Ed.; Metheuen & Co.: London, 1958.
(10) Hvidt, A.; Nielsen, S. O. *Adv. Protein Chem.* **1966**, *21*, 287–386.
(11) Karplus, M.; McCammon, J. A. *CRC Crit. Rev. Biochem.* **1981**, *9*, 293–349.
(12) Ernst, R. R. *Adv. Magn. Reson.* **1966**, *2*, 1–135.
(13) Ferrige, A. G.; Lindon, J. C. *J. Magn. Reson.* **1978**, *31*, 337–340.
(14) Neuman, R. C.; Jonas, V. *J. Am. Chem. Soc.* **1968**, *90*, 1970–1975.
(15) Van Geet, A., L. *Anal. Chem.* **1970**, *42*, 679–680.
(16) Roberts, G. C. K.; Jardetzky, O. *Adv. Protein Chem.* **1970**, *24*, 447–545.
(17) Wüthrich, K. In "NMR in Biological Research: Peptides and Proteins"; North-Holland: Amsterdam, 1976.

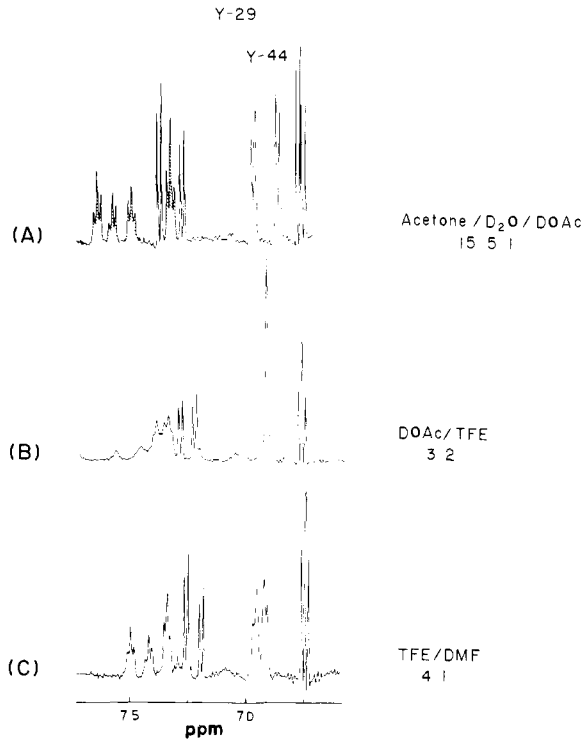


**Figure 2.** Aromatic proton NMR spectra of crambin: (A) in 15:5:1 deuterated acetone/water/acetic acid; (B) in 3:2 deuterated acetic acid/trifluoroethanol; (C) in 4:1 deuterated trifluoroethanol/dimethylformamide. Y-29 denotes $Tyr^{29}$ signals; Y-44 denotes $Tyr^{44}$ signals; $Phe^{13}$ resonances are hatched in A (spectra recorded at 600 MHz, ~298 K).

of the individual protons, as defined in a rigid configuration of the aromatic side chain, can vary widely.

$^1H$ NMR spectra of the aromatic region of crambin are shown in Figure 2 for the protein dissolved in the following deuterated solvents: 15:5:1 acetone/water/acetic acid (A), 3:2 acetic acid/trifluoroethanol (B), and 4:1 trifluoroethanol/dimethylformamide (C). The $Tyr^{29}$ side-chain resonances appear as a typical "random coil" doublet pair, at about 6.75 and 7.25 ppm, while the corresponding $Tyr^{44}$ signals are closer together, centered at about 6.95 ppm.[6,7] The doubling of signals from $Tyr^{29}$ need not concern us here: it stems from the compositional heterogeneities at sites 22 and 25 that perturb the environment of the aromatic protons.[6,7] Figure 2 confirms that while the $Tyr^{29}$ AA'XX' pattern is essentially independent of the nature of the solvent, such is not the case for $Tyr^{44}$ which exhibits two well-resolved doublets in A, a sharp singlet in B, and two partially overlapping doublets in C where, as in A, it exhibits an AA'BB' pattern. A temperature rise causes the $Tyr^{44}$ spectrum in 3:2 acetic acid/trifluoroethanol (B) to split and evolve toward a pattern such as seen in C, revealing that spectrum B results from an accidental degeneracy of the four-spin system. a similar trend is observed for the protein in 4:1 trifluoroethanol/dimethylformamide (C) where higher temperatures cause the two $Tyr^{44}$ doublets to move further apart. However, for the sample in 15:5:1 acetone/water/acetic acid, a solvent in which $Tyr^{44}$ exhibits a pattern (A) analogous to that in 4:1 trifluoroethanol/dimethylformamide (C), a temperature raise does not separate the doublets further but instead makes them converge toward the singlet pattern depicted in B. Therefore, simple inspection of the spectrum can lead to erroneous assignment of tyrosyl aromatic resonances since the pattern at a single temperature does not contain sufficient information to recognize the frequency ordering of the H2,6 and H3,5 signals. It follows that if a structure-destabilizing agent is allowed to act on the protein in a controlled fashion, so that the H2,6 and H3,5 resonances can be monitored as they shift from the "native" to the "random coil" pattern, the identity of the native form resonances should become evident from their spectral positions in the unfolded form. Clearly, temperature is one such agent when the transition is not entropically driven and, indeed, its effect

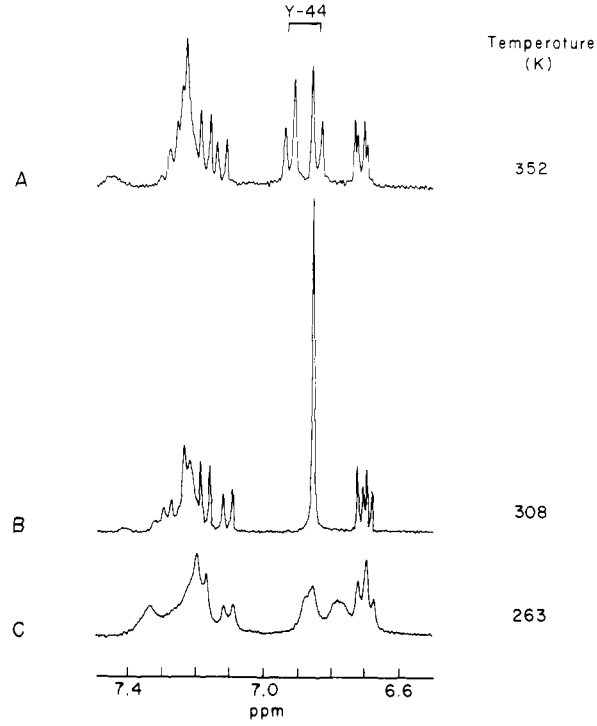


**Figure 3.** Proton NMR spectrum of crambin dissolved in 1:1 deuterated ethanol/acetic acid—temperature effect on the aromatic resonances: (A) 352 K; (B) 308 K; and (C) 263 K, (recorded at 300 MHz).

on the crambin spectrum has provided the criterion to distinguish tyrosyl ortho from meta doublets.[6]

The effects discussed above lead to another interesting conclusion: if a temperature rise leads to loosening and eventually to unfolding the structure,[6] then, as monitored by the $^1H$ NMR aromatic spectral pattern, solvent system A appears to be superior to B, which in turn would be better than C, in stabilizing the environment about the $Tyr^{44}$ side chain. In other words, the extent of conformational "opening" about the $Tyr^{44}$ ring site would appear to be modulated by the solvent composition.

Figure 3 illustrates the effect of temperature variation on the $Tyr^{44}$ spectral pattern for the protein dissolved in deuterated 1:1 ethanol/acetic acid. This solvent mixture is advantageous in that it enables cooling to 263 K, a temperature at which substantial broadening due to increased viscosity and possibly aggregation tends to overwhelm the spectral resolution. In this medium, the $Tyr^{44}$ H3,5 resonance is essentially temperature independent, appearing at ~6.87 ppm as the sample is heated from 263 to 352 K. In contrast, the H2,6 doublet moves from ~6.78 to ~6.93 ppm as the temperature is raised. At ~308 K the chemical shifts of the ortho and meta protons are identical and the coalesced, singlet pattern is generated. Crambin dissolved in 3:2 acetone/water yields very narrowed-line spectra so that temperatures as low as 233 K can be investigated. We have observed[7] that in this solvent coalescence of the two $Tyr^{44}$ doublets occurs at ~351 K. Plots of the $Tyr^{44}$ H2,3 and H3,5 chemical shifts vs. temperature for 3:2 acetone/water and for 1:1 ethanol/acetic acid are compared in Figure 4. As indicated, the coalescence temperature differs by ~40 K in the two solvents. Also depicted in Figure 4 is the trend for the protein in dimethylformamide, in which solvent cooling down to 296 K (the lowest temperature reached before freezing) provides no evidence of mergence for the $Tyr^{44}$ resonances. However, the coalescence temperature should not be given too much significance as it is determined by the temperature dependencies of both H2,6 and H3,5 chemical shifts. A thermodynamic analysis is required in order to judge the quality of a solvent in protecting the local conformation (see Dicussion).

In order to test for solvent perturbation effects on the $Tyr^{44}$ ring environment, the temperature dependence of $\Delta\delta = \delta_{H2,6} - \delta_{H3,5}$ (the chemical shift of the $Tyr^{44}$ phenolic H2,6 referred to that of its vicinal H3,5) was monitored in three solvents containing

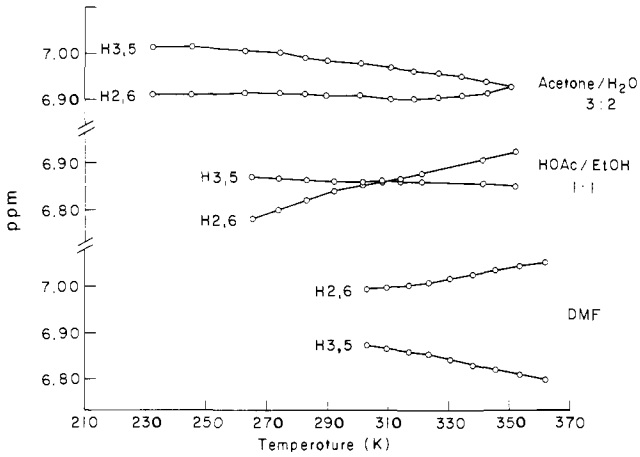


**Figure 4.** Solvent and temperature dependencies of the Tyr$^{44}$ aromatic proton NMR chemical shifts. Solvents: 3:2 deuterated acetone/water, 1:1 deuterated acetic acid/ethanol, and deuterated dimethylformamide.

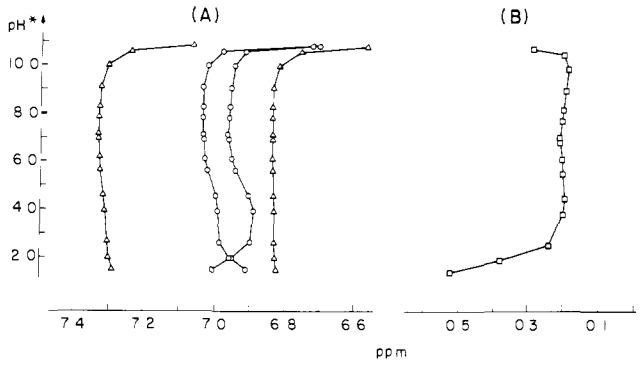


**Figure 5.** Acid–base titration of crambin: (A) pH* response of Tyr$^{44}$ ($\delta$ ~6.95 ppm) and Tyr$^{29}$ ($\delta$ ~7.3 ppm, H2,6, and $\delta$ ~6.8 ppm, H3,5) aromatic resonances; (B) pH* response of the Ile$^{33}$ $CH_3^{\delta}$ triplet (NMR spectra recorded at 300 MHz, ~298 K; solvent, 3:2 [$^2H_6$]acetone/$^2H_2O$).

trifluoroethanol. Coalesced resonances correspond to $\Delta\delta = 0$; $\Delta\delta > 0$ characterizes the more usual situation (i.e., the H2,6 doublet at lower field than the H3,5 doublet) while $\Delta\delta < 0$ represents "reversed" patterns (H2,6 doublet at higher field than the H3,5 doublet). Within the experimentally accessible temperature range and as far as can be extrapolated, $\Delta\delta > 0$ for crambin in trifluoroethanol, a situation similar to that encountered in dimethylformamide (Figure 4). A 2:3 trifluoroethanol/acetic acid mixture decreases $\Delta\delta$ to yield ortho–meta degeneracy at ~293 K and a definite pattern reversal at lower temperatures. More intriguing is the effect of a trace of dimethyl sulfoxide: at ~336 K, $\Delta\delta = +43$ Hz in pure trifluoroethanol and vanishes by adding dimethyl sulfoxide to 2% (v/v). At ~320 K, $\Delta\delta$ drops from 24 Hz in pure trifluoroethanol to −20 Hz in the perturbed solvent. Hence, we conclude that the Tyr$^{44}$ $^1$H NMR pattern is extremely sensitive to perturbations of the medium as a trace of dimethyl sulfoxide, itself a denaturing agent,[6] drastically enhances the properties of trifluoroethanol, a helix stabilizing solvent. How critical the effect is, is illustrated by our observation that minor hydration of the solvent mixture dramatically decreases the dimethyl sulfoxide induced stabilization.

A complication to be considered when dealing with solvents that involve Brønsted acids is that the proton activity changes upon mixing with a nucleophile such as dimethyl sulfoxide, so that the observed spectral changes can simply reflect acid–base titration of protein charged groups. To check for this effect, the $^1$H NMR spectrum of crambin dissolved in 3:2 acetone/water was monitored vs. pH*. Acid-base titration curves are shown in Figure 5A for both doublets of Tyr$^{44}$ (○) and the two doublets of Tyr$^{29}$ (△). As described above, in this solvent the Tyr$^{44}$ aromatic pattern appears "reversed" at ambient temperature and neutral pH. In fact, while the Tyr$^{29}$ resonances are practically insensitive to the acidity of the medium below pH* 10, the Tyr$^{44}$ resonances exhibit small

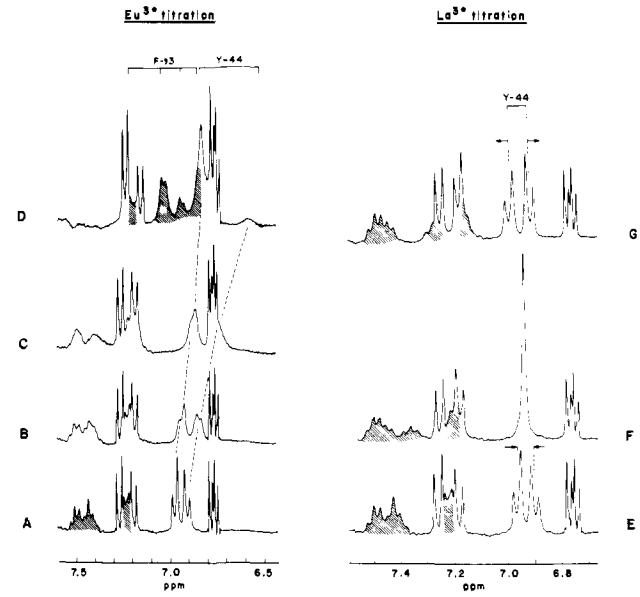


**Figure 6.** Proton NMR spectra of crambin at 300 MHz: lanthanide(3+) titration of the aromatic resonances. (A–D) Response to $EuCl_3$ additions: [$Eu^{3+}$]/[crambin] = 0.2 (B), 0.6 (C), and 3.0 (D). (E–G) Response to $LaCl_3$ additions: [$La^{3+}$]/[crambin] = 2 (F), and 11 (G). A and E are crambin spectra in the absence of lanthanide ions. Phe$^{13}$ resonances are hatched. Dashed lines (---) connecting spectra A, B, C, and D link Tyr$^{44}$ resonances. Arrows in spectra E and G indicate directions of resonance shifts induced by a temperature rise (solvent 3:1 [$^2H_6$]acetone/$^2H_2O$, pH* ~4.8, 298 K).

but definite shifts centered at pH* ~5. The crystallographic model (Figure 1) positions the Asp$^{43}$ $^{\gamma}COO^-$ adjacent to the Tyr$^{44}$ ring so that the pH effect most likely represents a response of the aromatic group to the titration of the neighbor carboxyl group (free group $pK_a$ ~ 4.5, in $H_2O$). As $^2$HCl is added, the doublets merge and reverse their ordering to assume the "normal" pattern below pH* ~2, the latter pH* representing the coalescence point. Thus, as expected, extreme acidity destabilizes the crambin structure which is sensed by the Tyr$^{44}$ ring. Pronounced shifts occur only at pH* >10 for both Tyr$^{29}$ and Tyr$^{44}$ due to titration of the phenol groups. In any event, the Tyr$^{44}$ doublet pattern reversal is observed at extremes of the pH scale, and the stabilizing effect of a trace of dimethyl sulfoxide is unlikely to arise from basification of the solvent as the amount of bulk trifluoroethanol ($pK_a$ ~ 12.4)[18] far exceeds the added nucleophile which, itself, is a weak base ($pK_b$ ~ 14, in $H_2O$).[19] One might speculate that a trace of dimethyl sulfoxide suffices to satisfy amide H-bonding requirements of exposed peptidyl bonds in crambin since, while trifluoroethanol is a good H-bond donor (Brønstead acid), dimethyl sulfoxide acts as an H-bond acceptor (Lewis base). On the other hand, methyl groups in dimethyl sulfoxide conceivably could stabilize exposed aliphatic groups on the protein surface through lipophilic interactions.

To investigate the Asp$^{43}$ side-chain effect on the Tyr$^{44}$ spectrum, crambin dissolved in 3:2 acetone/water was titrated with salts of 3+ lanthanide ions as it is well known[20] that these cations bind to exposed carboxyl groups. As illustrated in Figure 6, the Tyr$^{44}$ spectrum is most sensitive to the presence of $EuCl_3$, the presence to additions of the salt being consistent with binding of the shift reagent near the tyrosyl ring. At higher levels, $Eu^{3+}$ also causes an effect on Tyr$^{29}$ (Figure 6D) and on the Phe aromatic resonances (shown shaded in Figure 6A and D). The lanthanide titration curves for the tyrosyl ring resonances are presented in Figure 7. The Tyr$^{44}$ spectrum shifts following monotonically the $Eu^{3+}$ additions, the perturbation leveling at a [metal]/[crambin] ratio of ~1. At this point a response sets off for Tyr$^{29}$, reflecting titration of a second site. Consistently, titration with $PrCl_3$, another shift

(18) Llinās, M.; Klein, M. P. *J. Am. Chem. Soc.* **1975**, *97*, 4731–4737.
(19) Arnett, E. M. *Prog. Phys. Org. Chem.* **1963**, *1*, 223.
(20) Campbell, I. D., Dobson, C. M. & Williams R. J. P. *Proc. R. Soc. London, Ser. B* **1975**, *189*, 503–509.

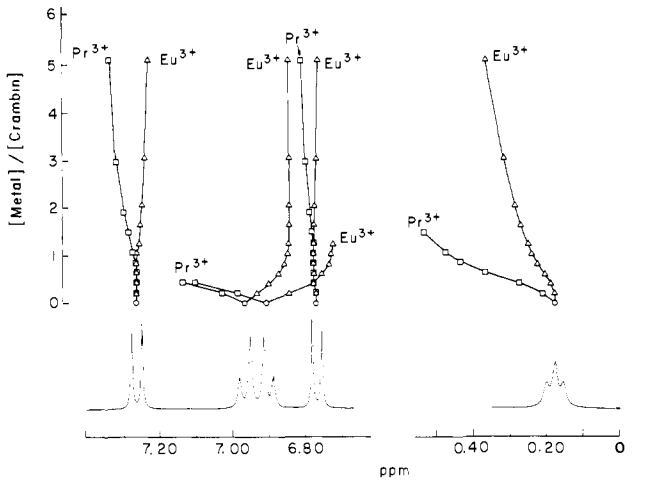


**Figure 7.** Effect of europium and praseodymium 3+ ions on the crambin $^1$H NMR spectrum: titration of selected resonances. Simulated resonances of the crambin spectrum at 300 MHz are included as reference: tyrosyl aromatic signals (left) and Ile$^{33}$ $CH_3^{\delta}$ triplet (right). The data were obtained from experiments such as illustrated in Figure 6: (□) $Pr^{3+}$, (△) $Eu^{3+}$.

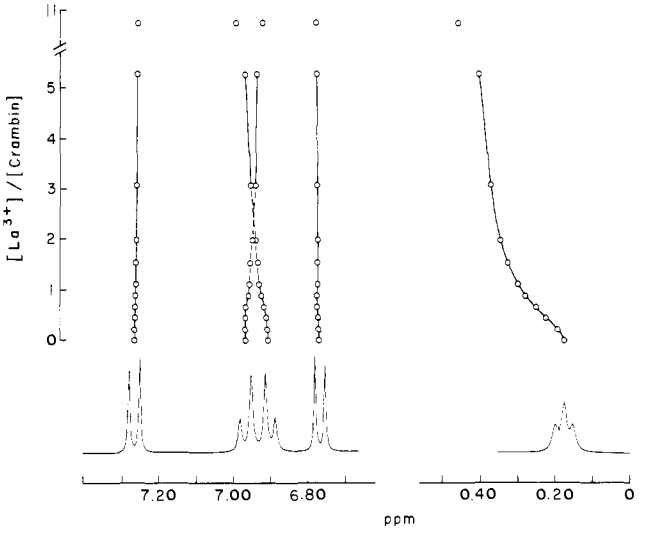


**Figure 8.** Effect of lanthanum 3+ ion on the crambin $^1$H NMR spectrum: titration of selected resonances. Simulated resonances of the crambin spectrum at 300 MHz are included as reference: tyrosyl aromatic signals (left) and Ile$^{33}$ $CH_3^{\delta}$ triplet (right). The data were obtained from the experiment illustrated in Figure 6.

reagent, affects the Tyr$^{44}$ pattern at once and perturbs the Tyr$^{29}$ aromatics only after the first site is saturated. The more pronounced effect of $Pr^{3+}$ compared to $Eu^{3+}$ can be ascribed to the larger hyperfine constant of the former relative to the latter (11 and −4, respectively[21]). An apparent association constant $K$ = 13 $mM^{-1}$ was determined for Eu(III) based on the titration profile of the Tyr$^{44}$ H3,5 protons. The second binding constant is much smaller; a value of ~0.1 $mM^{-1}$ is obtained for Pr(III) based on the H2,6 pair shift. This number, however, is affected by a larger uncertainly since the chemical shift of the bound species could not be determined accurately. The curve also presents a slight inflection which might indicate interaction between two sites. The crystallographic structure[4] shows that the three carboxylic groups of crambin lie on the surface of the protein but that the C terminus, Asn$^{46}$, is blocked owing to involvement in an intramolecular salt bridge to Arg$^{10}$. The NMR resuls agree well with the solid-state model in that the remaining carboxyls, belonging to Glu$^{23}$ and Asp$^{43}$ side chains, are neighbor to the aromatic rings of Tyr$^{29}$ and Phe$^{13}$ and of Tyr,$^{44}$ respectively (Figure 1).

The mechanisms by which $Eu^{3+}$ and $Pr^{3+}$ affect the crambin aromatic spectrum involve shift, relaxation, and possibly conformational phenomena that can obscure the intrinsic perturbations arising from the carboxyl–lanthanide complex. To discriminate against those effects, $La^{3+}$ was investigated, as it affords a diamagnetic analogue of similar binding specificity to that of $Eu^{3+}$ and $Pr^{3+}$. Figure 6E–G and 8 illustrate the effect of $La^{3+}$ on the Tyr$^{44}$ aromatic pattern; interestingly, metal binding to the first site causes only minor perturbation on the spectral pattern. However, for [metal]/[crambin] $\gtrsim$ 2, corresponding to a start of titration of the lower affinity site as detected by the onset of a small shift of the Tyr$^{29}$ resonance, the Tyr$^{44}$ doublets merge to a singlet and reverse to the "normal" (H2,6 low field, H3,5 high field) pattern. Thus, neither the acid–base shifts at pH* ~4.8 (Figure 5) nor the lanthanide titration experiments (Figure 7) support the view that the electrostatic field arising from the neighbor Asp$^{43}$ $\gamma$-carboxyl group determines the Tyr$^{44}$ side-chain resonance pattern. Furthermore, a structural destabilization of the protein conformation sets off at high lanthanum concentration (Figure 6), reminiscent of the acidity effect at pH* $\gtrsim$ 3 (Figure 5).

The crystallographic model of crambin[4] positions the Ile$^{33}$ side chain adjacent to the Tyr$^{44}$ ring (Figure 1B). In the $^1$H NMR spectrum, the Ile$^{33}$ $CH_3^{\delta}$ triplet appears shifted to higher fields by ~0.9 ppm, suggesting the proximity of an aromatic side chain that induces ring-current shifts. On the other hand, the 7.5-Hz breadth of the Ile$^{33}$ $CH_3^{\delta}$ resonance is considerably larger than 3.4 Hz, the average line width for the four other Ile triplets under the same external conditions.[22] This suggests a more efficient dipolar broadening for the Ile$^{33}$ $\delta$-methyl, presumably because of hindered rotation and close steric contact with the Tyr$^{44}$ ring which, in turn, would induce the observed anisotropic shift. This interpretaton is consistent with selective NOE experiments that show efficient magnetic cross-relaxation between the Ile$^{33}$ $\delta$-methyl and the Tyr$^{44}$ phenol spin systems.[6] The titration experiments discussed above reinforce such a model. Indeed, in 3:2 acetone/water the chemical shift of the Ile$^{33}$ $CH_3^{\delta}$ triplet decreases concomitantly to the freeing of the Tyr$^{44}$ ring as manifested by a reversal of its H2,6–H3,5 pattern at both extremes of the acidity scale (pH* $\gtrsim$10 and $\lesssim$3). Unlike Tyr$^{44}$ in the intermediate pH range, the $\delta$-methyl group shows only minimal pH response. This indicates that the Asp$^{43}$ titration which perturbs the Tyr$^{44}$ ring resonances does not affect the aromatic electron density distribution to the extent of modifying the shielding of the $CH_3^{\delta}$ group positioned at the other side of the ring (Figure 1B). The lanthanide titration studies also show that binding of rare earth ions deshields the Ile$^{33}$ triplet while destabilizing the Tyr$^{44}$ ring environment (Figure 7). As with the aromatic resonances, we observe a stronger spectral perturbation caused by $Pr^{3+}$ relative to that induced by $Eu^{3+}$. The sigmoid shape exhibited by the Ile$^{33}$ curve (Figures 7 and 8) might reflect a cooperative metal–protein interaction resulting from cation binding to more than one site, conceivably to Glu$^{23}$ in addition to Asp$^{43}$.

In 3:2 acetone/water the Ile$^{33}$ triplet appears at $\delta$ ~0.08 ppm, i.e., more shielded than in pure acetic acid in which solvent, at the same temperature, $\delta$ ~0.55 ppm.[22] In order to estimate the magnitude of the shifts caused by Tyr$^{44}$, calculations based on the crystallographic coordinates were performed according to the method proposed by Memory.[23] Shieldings of −0.41 and −0.22 ppm are predicted for the $\delta$ and $\gamma$ methyl groups of Ile$^{33}$, respectively. These values match well the experimental shifts of −0.42 and −0.16 ppm measured in acetic acid and indicate that in 3:2 acetone/water, where these shieldings are even larger, the Ile$^{33}$ side chain is probably closer to the Tyr$^{44}$ ring. Since in the mixed solvent the Tyr$^{44}$ aromatic spectral pattern is reversed from that in glacial acetic acid, the phenolic $\Delta\delta$ and the magnitude of the methyl chemical shifts appear to be related to each other, both reflecting the extent of structural stabilization of the pocket

(21) Bleaney, B., Dobson, C. M., Levine, B. A., Martin, R. B., Williams, R. J. P., & Xavier, A. V. *J. Chem. Soc., Chem. Commun.* **1972**, 791–793.

(22) Lecomte, J. T. J., De Marco, A. & Llinàs, M. *Biochim. Biophys. Acta* **1982**, *703*, 223–230.

(23) Memory, J. D. *J. Magn. Reson.* **1977**, *27*, 343–366.

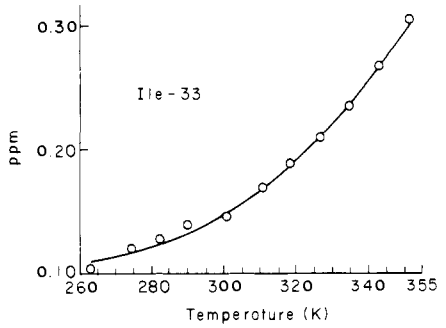


**Figure 9.** Temperature dependence of crambin Ile[33] δ-methyl triplet chemical shift. Experimental data points, marked by circles (o), were extracted from spectra at 300 MHz for the protein dissolved in 3:2 acetone/water, pH* ~5. The continuous curve was calculated on the basis of a two-state model (see text).

containing the Tyr[44] side chain (Figure 1C).

As in some of the investigated media crambin yields broadened spectra suggestive of aggregation, the contribution of such a process to our observations should be evaluated. We found that in pure dimethylformamide the proton spectrum is broad,[5,6] but when the protein is pretreated with glacial acetic acid[6] or when a trace of the acid (~1 μL) is added to the solution, the spectrum drastically sharpens without altering the pattern of the tyrosyl system. Moreover, the Tyr[29] NMR aromatic signals are negligibly perturbed by concentration and solvent changes despite the fact that the X-ray diffraction studies[4] show that in the crystal crambin exists as a dimer with intermolecular contacts involving the α-helix that contains Tyr[29]. Also, in two solvents that yield very narrow line spectra (3:2 acetone/water), Figure 2A, and 1:1 ethanol/acetic acid Figure 3B), Tyr[44] exhibits room-temperature spectral patterns unequivocally dissimilar. These lines of evidence indicate a negligible role for aggregation and a dominance of solvent effects in defining the Tyr[44] aromatic chemical shifts.

## Discussion

The effects described above are reminiscent of what has been observed in the process of thermal shift of the Ile[33] signal toward the "random coil" resonance position.[6] Assuming a two-state model that neglects states intermediate between "closed" and "open" structures, the observed chemical shift of a resonance that moves as a function of temperature, is given by

$$\delta_T = (\delta_c[\text{closed}]_T + \delta_o[\text{open}]_T)/[\text{protein}]$$

where $\delta_c$ ($\delta_o$) is the chemical shift of the closed (open) protein conformation, $[\text{closed}]_T$ ($[\text{open}]_T$) is the concentration of the closed (open) species at temperature $T$, and $[\text{protein}] = [\text{closed}]_T + [\text{open}]_T$. Formally, a temperature-dependent equilibrium constant may be defined as $K(T) = [\text{open}]_T/[\text{closed}]_T$; it follows that $K(T) = (\delta_c - \delta_T)/(\delta_T - \delta_o)$. The relative stabilization of open vs. closed states is expected to reflect protein interactions peculiar to each solvent system.

In order to calculate $K(T)$, $\delta_c$ and $\delta_o$ should be known. A reasonable initial estimate for $\delta_o$ is the reported "random coil" chemical shift for the amino acid residue in short polypeptide fragments.[24] A search was made for $\delta_c$ and $\delta_o$ values that minimize the error of the van't Hoff plot ln $K(T)$ vs. $T^{-1}$ and/or of the corresponding exponential form $K(T) = \exp[(\Delta S^{\text{eff}}/R) - (\Delta H^{\text{eff}}/RT)]$ from where values were obtained for $\Delta S^{\text{eff}}$ and $\Delta H^{\text{eff}}$, the "effective" entropy and enthalpy differences between the two states, respectively, in the various solvents.

An example of $\delta_T$ vs. $T$ plot for the Ile[33] $CH_3^{\delta}$ triplet in 3:2 acetone/water is given in Figure 9; the experimental data (o) were measured between 263 and 351 K. Such a temperature range enabled a good testing of the low-temperature limit chemical shift. The computer fit based on the two-state model gave a well-defined minimum of the quadratic error and accurate estimates of the asymptotic chemical shifts $\delta_o$ and $\delta_c$. The same sets of data for

(24) Bundi, A.; Wüthrich, K. *Biopolymers* **1979**, *18*, 285–297.

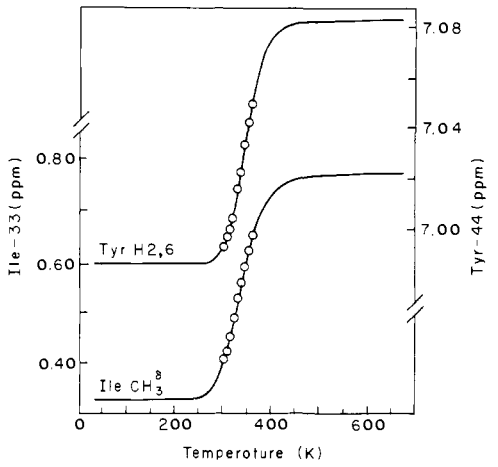


**Figure 10.** Temperature dependencies of crambin Tyr[44] phenol H2,6 and Ile[33] $CH_3^{\delta}$ chemical shifts. Experimental data points, marked by circles (o), were extracted from proton NMR spectra at 300 MHz for the protein dissolved in [$^2H_7$]dimethylformamide. The continuous curve was calculated on the basis of a two-state model (see text).

Table I. Thermodynamic Parameters for Crambin in Various Solvents

| resonance | $\delta_c$, ppm | $\delta_o$, ppm | $\Delta H^{\text{eff}}$, kJ·mol$^{-1}$ | $\Delta S^{\text{eff}}$, J·K$^{-1}$·mol$^{-1}$ | $T_c$, K |
|---|---|---|---|---|---|
| | | 3:2 Acetone/Water | | | |
| H2,6[a] | 6.907 | 7.173 | | | |
| H3,5[b] | 7.024 | 6.750 | 15.9 | 40.6 | 392 |
| $CH_3^{\delta}$[c] | 0.100 | 0.887 | 29.3 | 73.6 | 398 |
| | | 1:3 Acetic Acid/Ethanol | | | |
| H2,6 | 6.634 | 7.124 | 10.0 | 28.9 | 346 |
| H3,5 | 6.847 | 6.707 | | | |
| $CH_3^{\delta}$ | −0.023 | 0.970 | 12.1 | 33.5 | 361 |
| | | 1:1 Acetic Acid/Ethanol | | | |
| H2,6 | 6.620 | 7.127 | 10.0 | 31.0 | 323 |
| H3,5 | 6.874 | 6.720 | | | |
| $CH_3^{\delta}$ | −0.040 | 0.970 | 13.0 | 38.5 | 338 |
| | | 3:1 Acetic Acid/Ethanol | | | |
| H2,6 | 6.797 | 7.130 | 20.1 | 54.4 | 370 |
| H3,5 | 6.874 | 6.727 | | | |
| $CH_3^{\delta}$ | 0.167 | 0.986 | 19.2 | 54.0 | 356 |
| | | Acetic Acid | | | |
| H2,6 | 6.850 | 7.140 | 25.1 | 69.5 | 361 |
| H3,5 | 6.184 | 6.740 | | | |
| $CH_3^{\delta}$ | 0.290 | 0.970 | 20.1 | 57.7 | 348 |
| | | Trifluoroethanol | | | |
| H2,6 | 6.984 | 7.197 | 38.5 | 102.9 | 374 |
| H3,5 | 6.934 | 6.777 | | | |
| $CH_3^{\delta}$ | 0.513 | 0.970 | 41.0 | 114.6 | 358 |
| | | Dimethylformamide | | | |
| H2,6 | 6.984 | 7.080 | 51.1 | 147.7 | 346 |
| H3,5 | 6.890 | 6.717 | 34.7 | 97.5 | 356 |
| $CH_3^{\delta}$ | 0.327 | 0.773 | 39.7 | 118.0 | 337 |

[a] H2,6 aromatic doublet of Tyr[44]. [b] H3,5 aromatic doublet of Tyr[44]. [c] $CH_3^{\delta}$ triplet of Ile[33].

crambin dissolved in dimethylformamide is shown in Figure 10 which compares the Ile[33] response with that of Tyr[44]. Although the temperature range accessible for this solvent is narrower than for 3:2 acetone/water, the fitting of the experimental data was sensitive to the limit chemical shift parameters, and reliable values of the thermodynamic functions could be extracted.

Identified $\delta_o$ and $\delta_c$ values for the Tyr[44] H2,6 and H3,5 doublets and the Ile[33] $CH_3^{\delta}$ triplet, are listed in Table I and represented in Figure 11. In the case of Tyr[44], good initial estimates of $\delta_o$ are afforded by the Tyr[29] spectrum. Occasionally, the range of variation of the chemical shift from the "closed" to "open" conformation is narrow, making it difficult to determine accurately

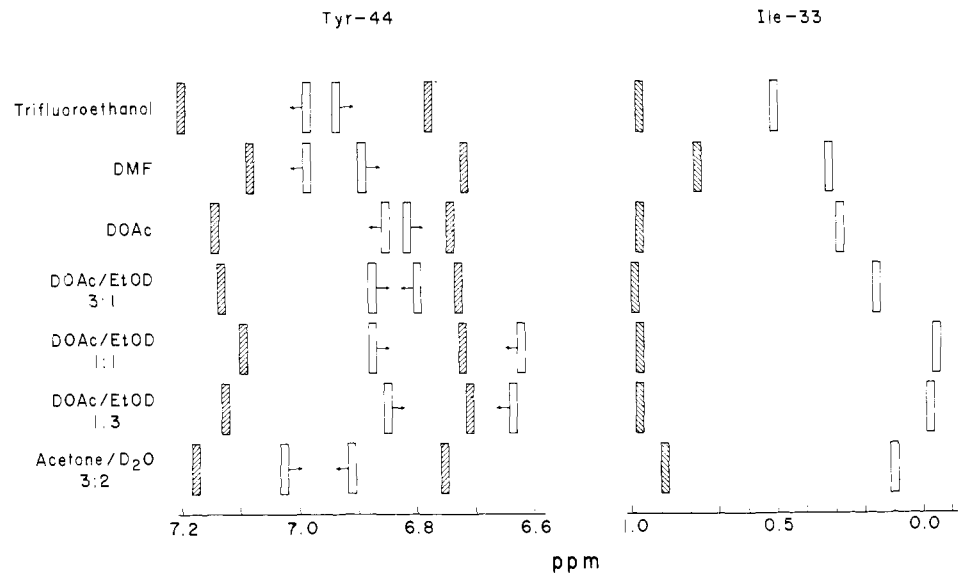


**Figure 11.** Limit chemical shifts of selected $^1H$ NMR resonances of crambin dissolved in various solvents. Hatched bars denote $\delta_o$, the optimal high-temperature limit chemical shift; blank bars denote $\delta_c$, the optimal low-temperature limit chemical shift. Arrows are used to indicate the direction of shifts induced by a temperature rise on the Tyr$^{44}$ resonances in the "closed" structural state. For Ile$^{33}$, the "random coil" value, 0.970 ppm, is arbitrarily assigned to $\delta_o$ in some solvent mixtures.

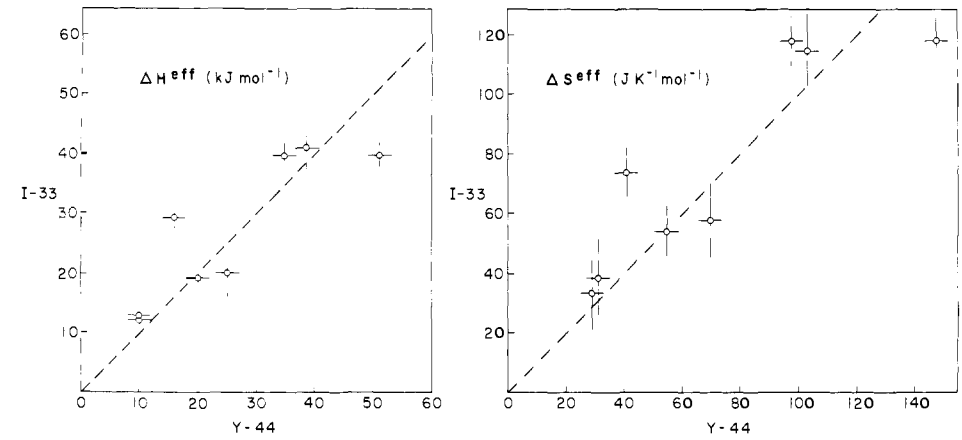


**Figure 12.** Calculated $\Delta H^{eff}$ and $\Delta S^{eff}$ values for crambin Ile$^{33}$ $\delta$-methyl and Tyr$^{44}$ aromatic H2,6 sites: correlation diagram. Each data point represents a different solvent system. Estimated uncertainties are indicated. The dashed lines are for an ideal, perfect correlation of the two groups.

the thermodynamic equilibrium functions; such was the case, e.g., for the Tyr$^{44}$ H3,5 in acetic acid. For some solvents, the methyl $\delta_o$ could not be identified reliably since the van't Hoff plots did not exhibit a well-defined error minimum upon variation of the parameter; in such cases a "random coil" value of 0.970 ppm was assumed for $\delta_o$.[24] Overall, it is apparent that the high-temperature limit $\delta_o$ varies less with solvent than does corresponding low-temperature parameter, $\delta_c$. For a given set of protons the shape of the calculated curves is strongly affected by the solvent composition. Thus, the simulated curves for the Tyr$^{44}$ ortho and meta resonances based on the experimental data for dimethylformamide show no trend toward crossing of the two doublets at any temperature, consistent with the experiment (Figure 4). Clearly, at a fixed temperature, the experimental Tyr$^{44}$ aromatic spectral pattern is dependent upon the asymptotic chemical shift values, $\delta_c$ and $\delta_o$, of *both* the H2,6 and H3,5 proton pairs.

$\Delta H^{eff}$ and $\Delta S^{eff}$ values determined by the procedure outlined above are listed in Table I. In most solvents, the thermodynamic functions for the Tyr$^{44}$ ring are very similar in magnitude to those derived for the Ile$^{33}$ methyl. Indeed, as illustrated by the $\delta$ vs. $T$ curves for dimethylformamide (Figure 10) the two sets of resonances typically move in parallel, a fact which, taking into account the structural proximity of the Ile$^{33}$ and Tyr$^{44}$ side chains (Figure 1C), suggests that Ile$^{33}$ is likely to contribute to determining the Tyr$^{44}$ chemical shifts as reflected by the extent of phenol spectral pattern reversal. $\Delta H^{eff}$ and $\Delta S^{eff}$ values for the Ile$^{33}$ $\delta$-methyl and Tyr$^{44}$ aromatic groups can best be compared from inspection of Figure 12 where dashed lines indicate the expected correspondence if the values of the thermodynamic functions were identical for the two groups.

One approach to estimating the stability of the environment of Tyr$^{44}$ is to resort to $T_c = \Delta H^{eff}/\Delta S^{eff}$, the compensation temperature. By definition, at this temperature $\Delta G^{eff} = 0$ so that the populations of the "closed" and "open" states are equal. However, as a measure of thermal stability, $T_c$ is rigorously applicable only to phenomena resulting from strong cooperativity; as discussed by Privalov,[25] events in the predenaturation temperature range that contribute to the protein heat capacity are not cooperative and therefore not expected to yield first-order transitions. With this reservation, the various solvent systems were classified according to their $T_c$ values as derived from Tyr$^{44}$ aromatic resonances; Figure 13 shows the ordering obtained on an increasing $T_c$ scale. Figure 13 also indicates the enthalpy gap $\Delta H^{eff}$ separating the two states. The following conclusions may be drawn (Figure 13): (a) $\Delta H^{eff}$ values derived from the phenolic H3,5 resonance for 3:2 acetone/water are similar to those for pure dimethylformamide, so that for these solvents $\Delta S^{eff}$ mainly is responsible for fixing their different $T_c$ values; (b) as exemplified by the data for dimethylformamide $\Delta H^{eff}$ and $\Delta S^{eff}$ values derived from H2,6 and H3,5 curves are similar, the small differences suggesting some structural stabilization about H2,6 protons, which are closer to the polypeptide backbone; (c) of all solvents tested,

(25) Privalov, P. L. *Adv. Protein Chem.* **1979**, *33*, 167–241.

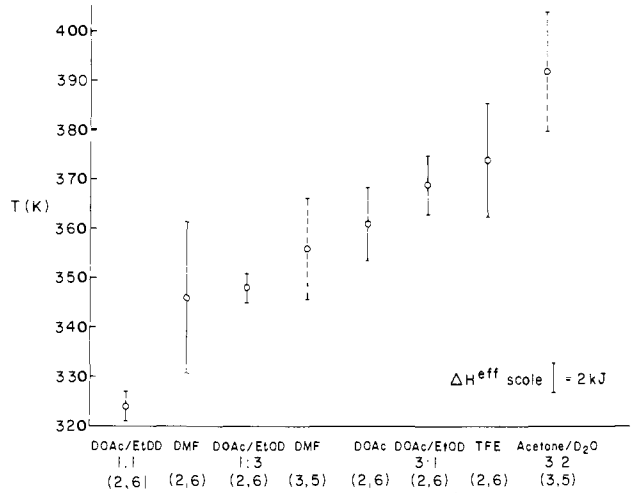


**Figure 13.** Compensation temperature, $T_c = \Delta H^{eff}/\Delta S^{eff}$, for crambin dissolved in various solvents. $T_c$ values are based on data and numerical fits for the $Tyr^{44}$ aromatic resonances. Vertical bars denote the enthalpy gaps, $\Delta H^{eff}$, separating "open" from "closed" states: continuous trace, data extracted from H2,6 resonances; broken trace, data extracted from H3,5 resonances.

3:2 acetone water is the best in terms of crambin structure stabilization (combined with its low intrinsic viscosity, this solvent mixture would appear to afford an optimal medium for NMR studies of crambin in solution). However, although the superiority of 3:2 acetone/water is satisfactorily predicted, the conclusions regarding the mixtures of ethanol and acetic acid do not correspond well with our observation that such solvents protect the $Tyr^{44}$ environment better than glacial acetic acid does. We attribute this insensitivity mainly to the approximations involved in the two-state model which, although convenient in terms of tractability, oversimplifies the dynamics.

## Conclusions

The protein structure is endowed with a number of degrees of freedom among which those that correspond to vibration, libration, and rotation variables are the most significant to characterize the internal motions. Recent theoretical modeling in terms of suitable potentials have yielded valuable dynamic pictures based on conventional normal mode representatons.[11] From such a standpoint, it is possible to energize thermally the vibrations leading to larger amplitudes of motion. At low temperatures, the molecule populates low-energy levels within harmonic potentials. As the temperature is raised to about 300 K the harmonic approximation becomes less valid,[11,26-28] and it ought to be expected that the rapid oscillations that average the chemical shifts will cause the latter to vary with temperature as these excited states no longer center on the normal modes' coordinates that correspond to minima of the potentials. Therefore, in the course of the NMR-detected thermal changes, the architecture of the protein does not vary in the sense that the conformation remains governed by the constraints that define the native state. At high enough temperature, eventual unfolding does occur, driving the protein to a "denatured" state that represents a totally different structure with its own set of internal forces and corresponding normal modes. The reversible transition from native to denatured states is highly cooperative process which for proteins of the size of crambin yields a relatively well-defined profile in an adiabatic scanning calorimetry experiment, the transition being centered at $T_m$, the melting temperature.[25] The processes discussed in this paper definitely do not correspond to such structural unfolding but rather reflect the thermally activated internal motions that are responsible for the intrinsic heat capacity of the protein in its native state.[25] In this view, the solvent effects as probed by, e.g., the $Tyr^{44}$ resonances, measure, at a constant temperature, the extent of anharmonicity (shape and shallowness) of the potentials as these are controlled by the environment. Upon changing solvents, the potentials change, and thence the thermostability of the protein globule as a whole.

The variety of NMR patterns displayed by $Tyr^{44}$ in crambin provides a valuable catalog of mobile Tyr ring spectra found in proteins. For example, reversed tyrosyl spectra have been observed for $Tyr^{21}$ in the basic pancreatic trypsin inhibitor,[29] $Tyr^{109}$ in the CB-9 fragments of troponin C[30], and $Tyr^{31}$ in the bovine pancreatic secretory inhibitor.[31] It is interesting that in a set of thionins, wheat and barley hydrophilic homologues of crambin that contain Tyr at site 13 and Phe at site 44 (instead of $Phe^{13}$ and $Tyr^{44}$ as found in crambin), the pattern of $Tyr^{13}$ in $^2H_2O$ solutions is close to, or exactly at, the coalescence point,[32] suggesting the presence of significant steric pressures on the site 13 residue as well.

In conclusion, the temperature-dependent chemical shifts of pairs of aromatic doublets from freely flipping tyrosyl rings are extremely sensitive to environmental factors and therefore able to provide insights into the micro-stability of tyrosine intramolecular niches.

**Acknowledgment.** The authors are thankful to Dr. H. L. Tookey for a generous supply of *Crambe abyssinica* seeds. This research was supported in part by the U.S. Public Health Service, NIH Grants GM-25213 and HL-29409. Purchase of the Bruker WM-300 NMR spectrometer was sponsored by the National Institutes of Health, Grant GM-27390. The 600-MHz NMR facility is supported by NIH Grant RR-00292.

**Registry No.** L-Tyrosine, 60-18-4; L-isoleucine, 73-32-5; L-aspartic acid, 56-84-8; L-phenylalanine, 7440-53-1; europium, 7440-53-1; praseodymium, 7439-91-0; lanthanum, 7439-91-0; acetone, 67-64-1; trifluoroethanol, 75-89-8; dimethylformamide, 64-17-5; ethanol, 64-17-5; acetic acid, 64-19-7.

(26) Mao, B.; Pear, M. R.; McCammon, J. A.; Northrup, S. H. *Biopolymers* **1982**, *21*, 1979–1989.
(27) Konnert, J. H.; Hendrickson, W. A. *Acta Crystallogr., Sect. A* **1980**, *36*, 344–350.
(28) Frauenfelder, H.; Petsko, M. R.; Tsernoglou, D. *Nature (London)* **1979**, *280*, 558–563.
(29) Snyder, H. G.; Rowan, R.; Sykes, B. D. *Biochemistry* **1976**, *15*, 2275–2283.
(30) Birnbaum, E. R.; Sykes, B. D. *Biochemistry* **1978**, *17*, 4965–4971.
(31) De Marco, A.; Menegatti, E.; Guarneri, M. *J. Biol. Chem.* **1982**, *257*, 8337–8342.
(32) Lecomte, J. T. J.; Jones, B. L., & Llinás, M. *Biochemistry* **1982**, *21*, 4843–4849.